Microscopic Evidence for the Modification of the Electronic Structure at Grain Boundaries of $Cu(In_{1-x}, Ga_x)Se_2$ Films

Doron Azulay, Isaac Balberg, and Oded Millo

Racah Institute of Physics and the Center for Nanoscience and Nanotechnology, The Hebrew University of Jerusalem, Jerusalem 91904, Israel

(Received 14 September 2011; published 14 February 2012)

We investigated the electronic properties around grain boundaries of polycrystalline $Cu(In_{1-x}, Ga_xSe_2)$ films as a function of Ga content, using scanning tunneling spectroscopy. Spectra acquired on samples with low Ga content ($x = 0$ and 0.33) reveal downward band bending with respect to adjacent p-type grains, suggesting type inversion at the surface of grain boundaries. Such a behavior was not observed for samples with high Ga contents. These results are consistent with our atomic force microscopy data and may shed light on the origin of the x-dependent efficiency for polycrystalline $Cu(In_{1-x}, Ga_xSe_2)$-based solar cells.

DOI: 10.1103/PhysRevLett.108.076603 PACS numbers: 72.40.+w, 68.37.Ef, 68.37.Ps

The electronic and optoelectronic properties of polycrystalline semiconductor systems usually differ from their single-crystal analogs because they are strongly influenced by the grain boundaries (GBs) formed between crystallites. Usually, the presence of GBs degrades solar-cell device performance due to defects and impurities that segregate there, creating in-gap electronic states that lead to enhanced recombination of photoexcited electron-hole pairs. However, in solar cells consisting of a chalcopyrite thin film absorber, it seems that the presence of GBs does not harm the device performance and may even help improve it. In particular, solar cells comprising a polycrystalline $Cu(In_{1-x}, Ga_x)Se_2$ (CIGSe) absorber seem to outperform their single-crystal counterpart, achieving a record solar energy conversion efficiency of ~20% [1]. This system includes a wide range of energy gaps depending on the Ga content, increasing from ~1.05 (for $x = 0$) to ~1.7 eV (for $x = 1$). The highest efficiency of polycrystalline-CIGSe-based solar cells is currently obtained for $x \approx 0.3$ [1].

In order to understand the possible role of GBs in affecting the performance of the above solar cells, various local probe microscopy techniques have been applied. Scanning Kelvin probe microscopy (SKPM) measurements on polycrystalline-CIGSe films showed a band bending at the GBs of up to 300 meV [2–4]. Our previous conductive atomic force microscopy (C-AFM) study [5] supports these findings and suggests also the presence of an additional valence-band offset as was calculated by Persson and Zunger [6]. A similar scenario was proposed by Hafemeister *et al.* [7] for $\Sigma 3$ GB. In order to check whether the band bending at GBs is beneficial to the photovoltaic performance, Jiang *et al.* measured such band bending as a function of the Ga content, by using SKPM, and correlated the results with the measured efficiencies of the corresponding cells [8]. They found that, while maintaining a nearly constant and relatively high GB band bending in the range $x = 0$–0.28, the efficiency of the device increased with Ga content, as expected from the band-gap increase with x. However, for higher Ga content the device efficiency decreased rapidly, although the gap is increasing. This efficiency reduction correlates well with the sharp decrease of the band bending that they found to take place in the $x = 0.28$–0.38 range. These authors concluded that the built-in potential at the GBs helps to improve the photocarrier collection efficiency, which is expected to improve device conversion efficiency [8].

Device simulations [9,10] show that a band bending at GBs due to charged defects can indeed improve the photogenerated carrier collection; however, this effect is hampered by the reduction in the open circuit voltage (V_{oc}), so that the overall efficiency of the device is consequently reduced. On the other hand, for neutral GBs with a valence-band offset larger than 300 meV, the simulated efficiencies were concluded to be similar to that of the single-crystal device. In all cases, however, the simulated efficiency of the polycrystalline-CIGSe-based solar cell never exceeded that of its single-crystal analog.

A recent scanning tunneling spectroscopy (STS) study [11] performed on CIGSe films with $x \approx 0.3$ showed spatial variations of the tunneling spectra near the GBs that can be explained by a combined effect of a downward band bending towards the GBs and an increased density of defect levels around the bottom of the conduction band. The spectra also indicate a reduced density of deep-level defects at the GBs that can yield low recombination activity. However, variations between different GBs in a particular sample and the dependence of the tunneling spectra on the Ga content were not addressed in that work. Following that, we present here direct evidence not only for band bending but also for type inversion at the GBs in similar CIGSe films. Our findings enable us to suggest a plausible reason for the efficient performance of the corresponding ($x \approx 0.3$ CIGSe) solar cells.

Our study consists of combined C-AFM and STS measurements of a series of polycrystalline $Cu(In_{1-x}, Ga_x)Se_2$ films having Ga contents that cover the whole range between $x = 0$ (CISe) and $x = 1$ (CGSe). The C-AFM data reveal band bending only for samples with $x \leq 0.5$ with average values that correlate well with the Ga-content dependence of the corresponding cell efficiencies. However, band bendings were observed only on part of the GBs. Our STS data manifest, with comparable abundance, GB band bending, exhibiting explicitly p- (grain surface) to n- (GB surface) type inversion for the $x = 0.33$ CIGSe films. The latter effect is quite significant, since it suggests that the minority carriers in the cells (i.e., the electrons) that are collected by the GBs enhance the efficiency of the cells.

The CIGSe samples were grown on Mo-coated float glass substrates using a multistage coevaporation process [12]. The scanning tunneling microscopy (STM) and AFM measurements were performed on the bare surface of the pure CIGSe absorber layer, with the underlying Mo layer serving as a back contact to the AFM or STM tip. The C-AFM measurements were performed in the contact mode using Ti/Pt-coated Si tips. Photo- and dark-current measurements were acquired simultaneously (along with the topography) under identical tip pressure (and thus similar electrical contact) by using a two-pass technique. In the first pass the current is measured along with the topography (with the AFM laser on, as required for the feedback), while the second current map is obtained promptly with the laser off, as detailed in Ref. [5]. Note that the wavelength of the AFM laser provides supra band-gap illumination ($\sim$ 650 nm) with an effective intensity of about 100 $\frac{\text{mW}}{\text{cm}^2}$ [5].

The STM measurements presented here were performed at room temperature, in the dark, and in vacuum ($\sim 10^{-6}$ Torr). Prior to these measurements, the samples were treated for 2 min in an aqueous KCN solution (5%) to remove surface oxidation. The samples were washed then with distilled water, dried, and inserted rapidly (about 2 min exposure to air) into the STM chamber that was promptly evacuated. The STM topographic images were typically measured with sample-bias and current set values of $V = 1.5$ V and $I = 1$ nA, whereas the tunneling I-V curves were acquired with set values (before disabling the feedback loop for spectrum acquisition) of $V = 0.8$ V and $I = 0.5$ nA. Our dI/dV-V tunneling spectra, which are proportional to the local density of states (DOS) [13], were numerically derived from curves resulting by averaging over 15–25 I-V characteristics taken at a specific location, in each of which the current was recorded, and averaged over, 64 times for every bias value.

Figure 1 shows a typical C-AFM topography, dark- and photocurrent maps measured simultaneously at $V =$ 50 mV (sample bias) on a CIGSe film with $x = 0.33$. The currents are mainly along the GBs but not through

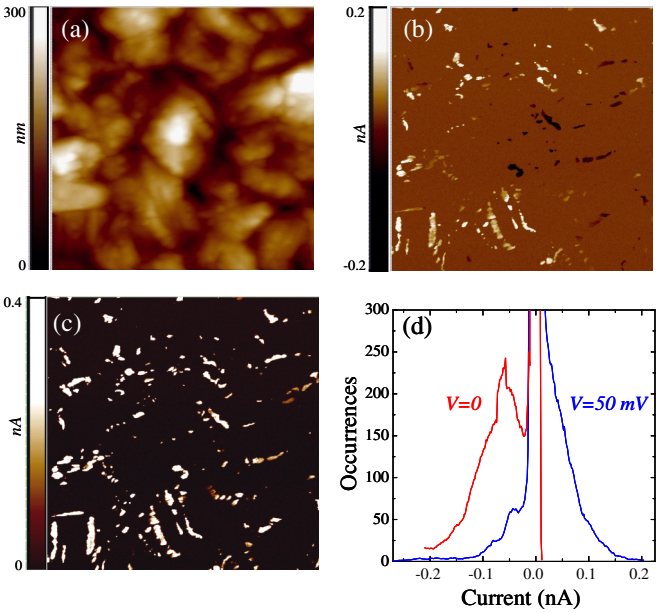

FIG. 1 (color online). Topography (a), photocurrent (b), and dark-current (c) maps measured on an $x = 0.33$ CIGSe film with 50 mV bias voltage. Scan size: 4×4 μm^2. (d) The photocurrent histograms at zero bias (red) and at 50 mV (blue), showing that the reversed photocurrent vanishes (on average) at $\sim$50 mV.

all of them. In the dark [Fig. 1(c)], only positive currents are observed, as expected. However, the current map measured under illumination [Fig. 1(b)] shows negative currents in some of the GBs (flowing counter to the applied bias) and positive in others. At much lower bias values only negative photocurrents were detected along the GBs, as demonstrated by the $V = 0$ photocurrent histogram presented in Fig. 1(d), while at much higher bias values only positive currents were observed. The crossover bias voltage V_c, at which the mean of the current distribution becomes zero, is a measure of the band bending at the GBs [5], as is shown to be the case of 50 mV for the $x = 0.33$ sample [see Fig. 1(d)]. It should be noted, however, that this value provides a *lower limit* to the band bending, due to the background contribution of the forward current at the GBs.

Figure 2(a) portrays the average V_c (taken over many GBs that showed downward band banding) as a function of the Ga content. It is seen that, for Ga contents above $x = 0.33$, there is a sharp reduction of V_c towards zero. In Fig. 2(b), we present the efficiency (η) of the reference solar cells as a function of the absorber's Ga content. The efficiency initially rises with Ga content, as expected from the corresponding increase of the band gap, but it drops sharply for higher Ga contents ($x \geq 0.5$) due to the suppression of the short-circuit current I_{sc}. These results are in agreement with Ref. [8] and suggest that the band bending at GBs, observed in both SKPM and C-AFM experiments, may aid photocarrier collection in the cells. We should remark, however, that we have observed dark or

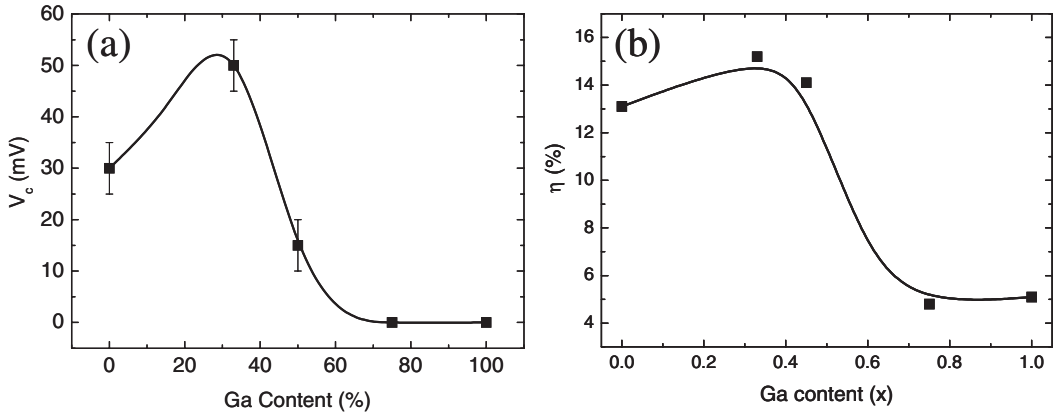

FIG. 2. (a) Average V_c as a function of the Ga content x. (b) The device efficiency of the reference solar cells. The error bars reflect the spread in the measurements, and the lines are guides to the eye.

photocurrent only on part of the grain boundaries. This observation can be related to the SKPM results reported by Baier *et al.* [14], where some GBs showed upwards rather than downwards band bending. It may well be that current can be measured (in the applied bias range) only on the latter GBs, and obviously no negative currents can be detected in GBs showing upwards band bending. It should be noted, however, that SKPM is a pure surface sensitive technique, while the current maps measured by C-AFM are affected also by the transport properties and charge photogeneration in the bulk. We therefore turned to apply STS, a surface sensitive technique, to gain further insight into possible variations among GBs within a sample. STS is particular appealing for our study, since it can also monitor conduction and valence-band offsets at the nano scale [15] and even provide direct evidence for n-type to p-type inversion [16].

In Fig. 3, we show typical results as obtained for samples with three Ga contents. For each x, two tunneling spectra are presented, one acquired on a GB and the other on an adjacent grain, as indicated in the topographic images shown to the left. Two conspicuous features are to be noted. For the $x = 0.33$ sample, the spectrum acquired on the GB is clearly shifted towards negative bias with respect to that taken on the grain, consistent with a downwards band bending at the GB. Importantly, the spectrum measured on the GB exhibits a clear depression in the DOS, much more pronounced than that observed on the adjacent grain. A similar depression was reported in Ref. [11], but here it is centered at around $V = -220$ mV rather than at zero bias. Concomitantly, the chemical potential ($V = 0$) at this GB is located at a voltage where the DOS clearly rises towards the conduction band edge, in vast contrast to the behavior in the adjacent grain. It is hard to estimate from the spectral shift, as evident as it may be, the actual value of the band bending, since the tunneling spectra do not easily lend themselves to an exact determination of the band edges. The spectra are largely affected, in particular, at elevated bias voltages, by unknown factors such as the density of shallow defect levels and the bias-dependent tunneling barrier. The most reliable estimate for the band-bending value is then the shift of the DOS minimum, implying band bending of ~200 meV. Spatial spectral shifts such as that shown by Fig. 3(d) were found for about 50% of the grain-GB pairs measured on the $x = 0.33$ sample, showing shifts of the DOS minima in the range 100—230 meV. By adopting the band-diagram scheme presented in Ref. [11], such shifts are sufficient for driving the GBs to become n-type at their surface. We would like to point out that we have never observed spectral shifts towards positive bias, in contrast to the positive band bending found on some GBs in a recent SKPM experiment [14].

A similar behavior, yet only on about 25% of the measured GBs, was observed also on the $x = 0$ (CISe) film, as portrayed by the spectra plotted in Fig. 3(b). Here, the DOS minimum at the GB is shifted to -120 mV. The origin of the shoulder in the 0–300 mV range is not yet clear, and it may reflect an increase in the density of shallow defects around the conduction band edge. This feature, however, was not observed for all GBs.

In contrast to the $x = 0$ and $x = 0.33$ samples, we never observed any spectral or DOS minima shifts for the $x = 0.75$ and $x = 1$ (CGSe) films. In Fig. 3(f), we show a typical pair of dI/dV-V tunneling spectra acquired on a GB and adjacent grain on an $x = 0.75$ sample. The two spectra appear to be nearly identical up to a bias of ≈ 0.3 V, above which the slope of the spectrum measured on the grain becomes larger than that on the GB. This effect does not necessarily imply an increased DOS on the grains at elevated energies and may be due to a smaller tunneling barrier (e.g., a smaller work function or electron affinity) on the grain. This particular feature was not generic, and some pairs of spectra were nearly identical over a wider voltage range. However, as noted above, no shift in the DOS minima was observed in any of such pairs of spectra measured over tens of grain-GB pairs for the CGSe and $x = 0.75$ CIGSe films.

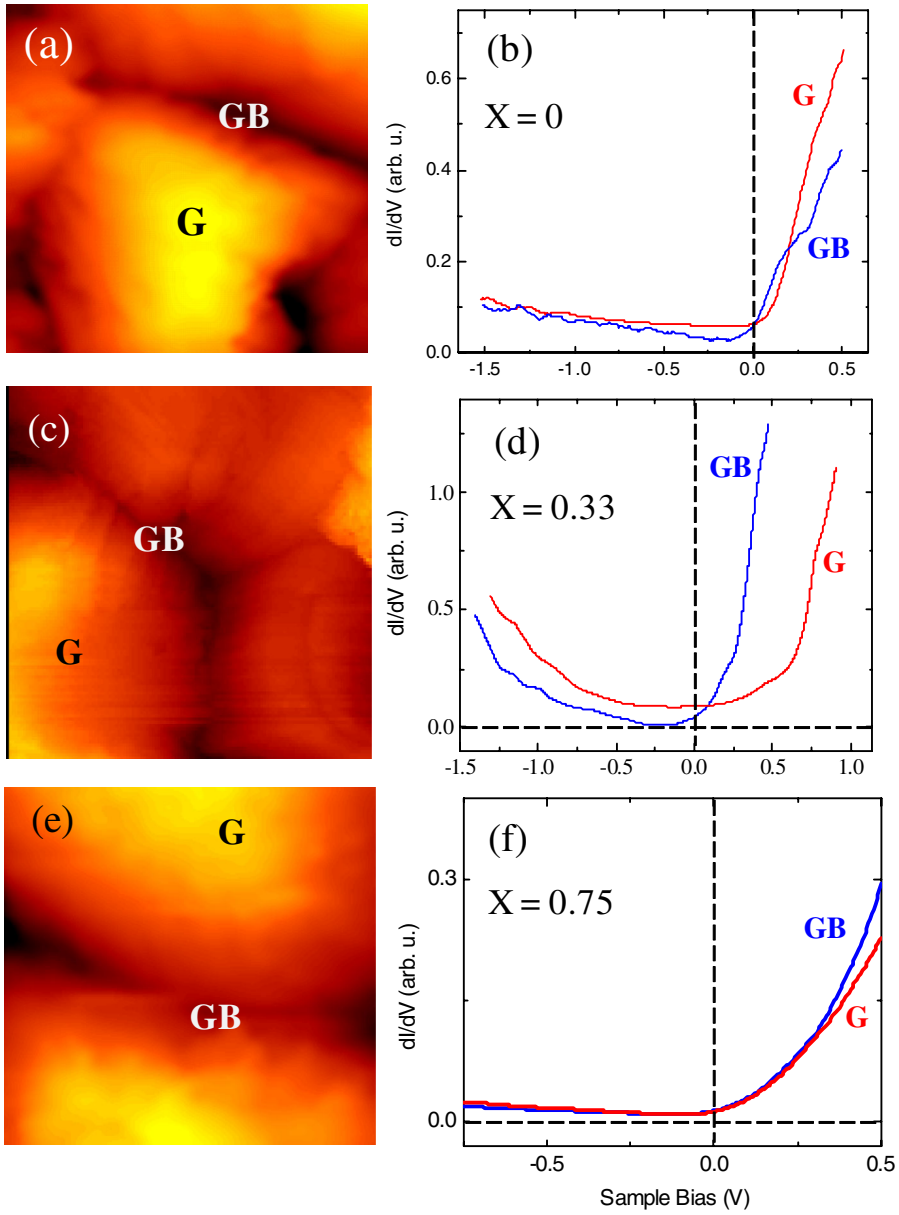

FIG. 3 (color online). 0.5×0.5 μm^2 STM topographic images measured on CIGSe films with $x = 0$ (a), $x = 0.33$ (c), and $x = 0.75$ (e) and corresponding tunneling spectra (b), (d), and (f) measured on grain centers (red curves, "G") and grain boundaries (blue curves, "GB") at positions indicated in the respective images. The spectra presented in (d) exhibit a pronounced spectral shift, manifesting downwards band bending at GBs to a degree that yields type inversion, from p-type (on grain) to n-type (on the GB). The above spectra manifest also reduced DOS at around the band center at the GB with respect to the adjacent grain. In contrast, neither a spectral shift nor a reduction in the GB DOS at the chemical potential is observed for $x = 0.75$ (f). Note that the plots have different scales.

As mentioned above, the spectra shown in Fig. 3(d) for $x = 0.33$ were found at about 50% of the GBs. Other GBs exhibited the behavior shown in Fig. 4. The spectra measured on these GBs exhibit a notable dip centered around zero bias, in contrast to those measured on the center of the adjacent grains that exhibit a very shallow dip. These data thus manifest a significantly reduced DOS at the chemical potential of the GB with respect to that of the grain center. Such a behavior (and in fact very similar spectral features) was reported by Mönig *et al.* for $x = 0.3$ [11]. As pointed out by these authors, the reduced density of deep-level defects at the GBs, as manifested by these spectra, imply a low recombination rate at GBs, which is beneficial for solar-cell operation. However, the spectra presented in Fig. 4 do not portray an explicit signature for band bending or type inversion at the GBs, an effect that assists charge separation.

Our STS and C-AFM data are in good agreement with one another, in particular, when noting that V_c (see Fig. 2) provides only a lower limit to the band bending. Both types

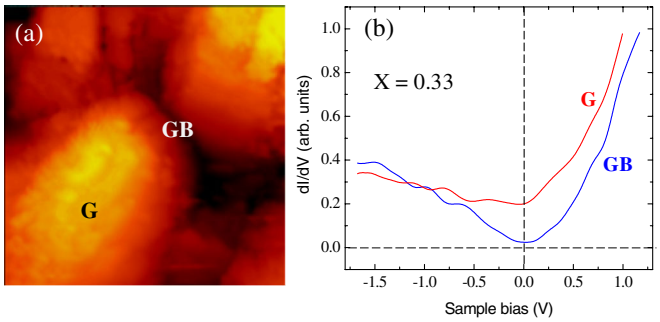

FIG. 4 (color online). (a) $0.5 \times 0.5\ \mu m^2$ STM topographic image measured on a CIGSe film with $x = 0.33$. (b) Two tunneling spectra, one measured on the grain center (red curve, G) and the other on the grain boundary (blue curve, GB), at positions indicated in the topographic image. A reduced DOS around the chemical potential is observed at the GB, but no clear signature for band shifts (band bending) is detected on this GB.

of measurements reveal band bending at GBs only for the low Ga-content samples, with no signature of such an effect for CIGSe films with $x > 0.5$. It should be noted that such good agreement is by no means trivial, since, unlike STS, the C-AFM results are affected also by the bulk. More importantly, our tunneling spectra provide evidence that the band bending may yield type inversion at the GB surface (which should also extend somewhat into the GB interior), namely, that they have n-type character. Recent scanning capacitance measurements also suggest such type inversion at the GBs of similar samples [17]. It is important to note here that type inversion in GBs is assumed to be an important ingredient in enhancing the efficiency of polycrystalline-CIGSe-based solar cells, due to its possible contribution to the minority-carrier collection.

Another important observation provided by our local probe measurement is the variation in the electronic properties among GBs within the same sample. In particular, both STS and C-AFM data show that band bending takes place only at ~50% of GBs on the $x = 0.33$ sample and less abundantly for the $x = 0$ and $x = 0.5$ samples (25%–30% and ~10%, respectively). This behavior may also have consequences related to the performance of polycrystalline-CIGSe-based solar-cell devices. Band bending at GBs improves the minority-carrier collection and, consequently, increases I_{sc}. At the same time, however, the recombination current along such GBs acts to decrease the open circuit voltage V_{oc}. Simulations show that the latter effect dominates, and the device efficiency should thus reduce [2,9,10]. It may be then that the fact that only part of the GBs' surface exhibit significant band bending on the CIGSe films should be beneficial for the cell performance, allowing, on the one hand, a better collection efficiency with respect to the single-crystal cell yet not hampering too much the V_{oc}, on the other hand.

In summary, direct evidence for band bending at grain boundaries of polycrystalline-CIGSe films, to an extent that may drive the surface of GBs to become n-type, is provided by scanning tunneling spectroscopy. Such a behavior was observed only for films with low Ga content, $x = 0$ and 0.33, but not for $x = 0.75$ and 1. These findings are consistent with C-AFM data obtained on the same films that exhibited band bending only for $x < 0.5$. The good correlation between the Ga-content dependence of the band bending and the efficiency of CIGSe-based solar cells points to the important effect the GBs have on the solar-cell performance. In particular, the (p- to n-) type inversion at the GBs surface observed in our tunneling spectra, most clearly for the $x = 0.33$ film, appears to be a key contributor to the maximal efficiency that was found for solar cells consisting of $x \approx 0.3$ polycrystalline-Cu$(In_{1-x}, Ga_x)Se_2$ absorbers. This follows the expected relatively efficient minority-carrier collection in the GBs.

The authors thank Th. Rissom (Helmholtz-Zentrum Berlin) for sample growth and D. Abou-Ras and S. Sadewasser (Helmholtz-Zentrum Berlin) for very helpful discussions. This work was supported by grants from the Federal Ministry for the Environment, Nature Conservation and Nuclear Safety (BMU) under Contract No. 0327559H, the Israel Science Foundation, and the Wolfson Foundation. I. B. acknowledges the support of the Enrique Berman chair in Solar Energy Research at the HU and O. M. acknowledges the support of the Harry De Jur Chair of Applied Science at the HU.

[1] P. Jackson *et al.*, Prog. Photovoltaics **19**, 894 (2011).
[2] U. Rau, K. Taretto, and S. Siebentritt, Appl. Phys. A **96**, 221 (2009).
[3] S. Sadewasser *et al.*, Thin Solid Films **431**, 257 (2003).
[4] G. Hanna *et al.*, Appl. Phys. A **82**, 1 (2006).
[5] D. Azulay *et al.*, Solar Energy Mater. Sol. Cells **91**, 85 (2007).
[6] C. Persson and A. Zunger, Phys. Rev. Lett. **91**, 266401 (2003).
[7] M. Hafemeister *et al.*, Phys. Rev. Lett. **104**, 196602 (2010).
[8] C.-S. Jiang *et al.*, Appl. Phys. Lett. **85**, 2625 (2004).
[9] W. Metzger and M. Gloeckler, J. Appl. Phys. **98**, 063701 (2005).
[10] K. Taretto and U. Rau, J. Appl. Phys. **103**, 094523 (2008).
[11] H. Mönig *et al.*, Phys. Rev. Lett. **105**, 116802 (2010).
[12] C. Kaufmann *et al.*, Solar Energy Mater. Sol. Cells **93**, 859 (2009).
[13] R. Wiesendanger, *Scanning Probe Microscopy and Spectroscopy* (Cambridge University Press, London, 1994).
[14] R. Baier *et al.* (to be published).
[15] D. Steiner *et al.*, Nano Lett. **8**, 2954 (2008).
[16] D. Mocatta *et al.*, Science **332**, 77 (2011).
[17] W. Li, S. R. Cohen, and D. Cahen, IEEE J. Photovoltaics (to be published).